Measurement of Larmor precession angles of tunneling neutrons

Masahiro Hino,[1] Norio Achiwa,[2] Seiji Tasaki,[1] Toru Ebisawa,[1] Takeshi Kawai,[1] Tsunekazu Akiyoshi,[1] and Dai Yamazaki[3]
[1]*Research Reactor Institute, Kyoto University, Osaka 590-0494, Japan*
[2]*Department of Physics, Kyushu University, Fukuoka 812-8581, Japan*
[3]*Department of Nuclear Engineering, Kyoto University, Kyoto 606-8501, Japan*
(Received 26 February 1998; revised manuscript received 2 November 1998)

We have succeeded in measuring precisely the spin precession angle of neutrons tunneling through a Permalloy45 ($Fe_{55}Ni_{45}$) ferromagnetic film as a function of incident angles. The angles of additional spin precession are directly observed as a shift of neutron spin echo (NSE) signals by inserting the film in one of the Larmor precession fields of a transverse NSE spectrometer, and are well reproduced by the relative phase difference between ↑ and ↓ spin neutron wave functions, which are derived by solving the one-dimensional Schrödinger equation for the optical potentials in the film. The Larmor times are extracted from the additional spin-precession angles for nontunneling and tunneling cases. [S1050-2947(99)07403-X]

PACS number(s): 03.75.Dg, 73.40.Gk

I. INTRODUCTION

In recent years there has been considerable interest in the tunneling time (cf. the reviews and references therein [1–5]). The question of tunneling time is often a focus of controversy although it seems not so complex. A variety of definitions have been introduced and there still is a lack of consensus on the existence of a unique expression for the time scale.

Among these definitions, a proposal for measuring the tunneling time using the Larmor clock [1,6,7] has a chance of being implemented by experiments. This idea is to measure Larmor precession of a particle that is caused by a weak magnetic field within the classically forbidden potential barrier. The time is defined by dividing the angle of spin precession Ω with the Larmor frequency ω_L in the magnetic field, and it is called local Larmor time $\tau=\Omega/\omega_L$ [3,6,7]. The Larmor clock has been criticized [3] and there is still discussion as to the meaning of the Larmor time for the tunneling case. A few experiments were performed concerning the Larmor time with tunneling electrons or a light beam [8–10]. No experiment with tunneling neutrons has been reported, to our knowledge, except for our previous works [11,12], though neutron is one of the best candidates for measuring the Larmor time due to its characteristics; spin angular momentum, zero net charge, and heavy mass as compared with the electron.

In the previous works, we have performed to measure additional Larmor precession angles of neutrons transmitted through a magnetic film at various incident angles across the critical angle of total reflection for ↑ spin with a configuration of an neutron spin echo (NSE) spectrometer [13]. The state of Larmor precession is represented as a coherent superposition of eigenstates of ↑- and ↓- spin neutrons [14,15]. The Larmor precession angle is interpreted as a relative phase difference of ↑ and ↓ spin neutron wave functions. However, the previous experimental data of the additional spin precession angles indicated a little deviation in the tunneling region, in comparison with the theoretical spin precession angle (the relative phase difference) based on one-dimensional rectangular magnetic model.

Therefore, the purposes of this paper are (1) to measure precisely the additional spin precession of neutron tunneling through the magnetic film at various incident angles from the nontunneling to tunneling region for both ↑ and ↓ spins, (2) to compare the measured additional precession angle with the relative phase difference of ↑ and ↓ spin neutron wave functions derived by solving the one-dimensional Schrödinger equation, and (3) to extract Larmor times of nontunneling and tunneling neutrons from the additional spin precession angles, and discuss the validity of these Larmor times as a time that these neutrons spend in the film.

II. BASIC THEORY

A. Larmor precession of neutron through a magnetic thin film

As shown in Fig. 1, refraction and reflection of a neutron beam at a surface of a magnetized film are considered as problems of a rectangular potential barrier in a one-dimensional Schrödinger equation [16–18]. In a magnetic

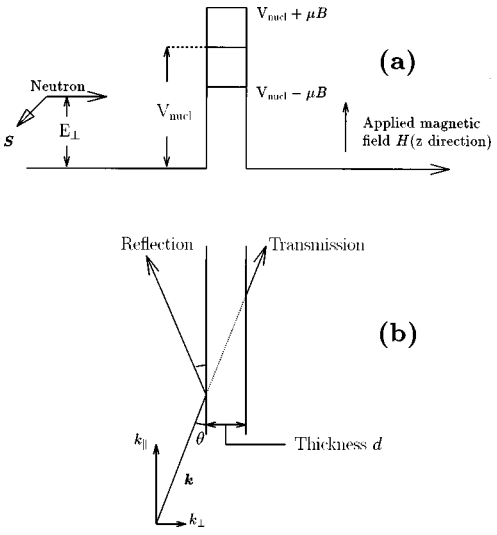

FIG. 1. (a) The potential energy and (b) schematic view for a Larmor precessing neutron entering into a magnetic film at an incident angle θ.

film, the average nuclear and magnetic potential are given by $V_{\rm nucl}=(2\pi\hbar^2/m_{\rm n})\rho b_{\rm coh}$ and μB, respectively. $m_{\rm n},\mu$ are the neutron mass and the value of neutron magnetic moment, respectively, and $\rho, b_{\rm coh}, B$ are the number density of atoms, the average coherent scattering length, the magnetic induction, in the film, respectively. In general the scattering length $b_{\rm coh}$ is complex, but the effective imaginary part is 10^{-4} or smaller coherent part ($V_{\rm nucl}$) in this sample. Therefore the imaginary part is negligible.

Let us consider the spin precession of neutron tunneling through the magnetic film. In the transmission process of neutron through the magnetic film, the Hamiltonian is diagonal and the direction of quantization axis does not change. Therefore the Schrödinger equation can be solved separately for both $\hbar/2$ and $-\hbar/2$ spin cases. The transmitted stationary wave function is described as

$$|\psi_{\pm}(y)\rangle = D_{\pm}e^{iky}, \tag{2.1}$$

where $k=\sqrt{2m_{\rm n}E_{\perp}}/\hbar, k$ is the normal component of wave vector in vacuum (air). The amplitudes of the transmitted wave through the film with thickness d are obtained as [1,11]

$$D_{\pm}=T_{\pm}^{1/2}e^{i\Delta\phi_{\pm}}e^{-ikd}e^{\mp(i\delta/2)}, \tag{2.2}$$

where $\kappa_{\pm}=\sqrt{2m_{\rm n}(V_{\rm nucl}\pm\mu B-E_{\perp})}/\hbar;\kappa$ and δ are the normal components of the wave vector in the tunneling region of the film and the incident Larmor precession angle at surface of the film, respectively. The subscripts $+$ and $-$ indicate the neutrons of $\uparrow$ and $\downarrow$ spin, respectively. Here $T_{\pm}$ are transmission probabilities of $\uparrow$ and $\downarrow$ spin neutrons tunneling through the film and are given by

$$T_{\pm}=\left(1+\frac{(k^2+\kappa_{\pm}^2)^2}{4k^2\kappa_{\pm}^2}\sinh^2(\kappa_{\pm}d)\right)^{-1}. \tag{2.3}$$

The additional phases of $\uparrow$ and $\downarrow$ spin neutrons tunneling through the magnetic film, $\Delta\phi_{\pm}$, are determined by

$$\tan(\Delta\phi_{\pm})=\frac{k^2-\kappa_{\pm}^2}{2k\kappa_{\pm}}\tanh(\kappa_{\pm}d). \tag{2.4}$$

The expectation value of neutron transmitted through the film $\langle S_{\rm x};{\rm tr}\rangle, \langle S_{\rm y};{\rm tr}\rangle$ and $\langle S_{\rm z};{\rm tr}\rangle$ are given by

$$\langle S_{\rm x};{\rm tr}\rangle=\hbar\cos(\Delta\phi_{+}-\Delta\phi_{-}-\delta)\frac{\sqrt{T_{+}T_{-}}}{T_{+}+T_{-}}, \tag{2.5}$$

$$\langle S_{\rm y};{\rm tr}\rangle=-\hbar\sin(\Delta\phi_{+}-\Delta\phi_{-}-\delta)\frac{\sqrt{T_{+}T_{-}}}{T_{+}+T_{-}}, \tag{2.6}$$

$$\langle S_{\rm z};{\rm tr}\rangle=\frac{\hbar}{2}\frac{T_{+}-T_{-}}{T_{+}+T_{-}}. \tag{2.7}$$

This relative phase difference $\Delta\phi_{+}-\Delta\phi_{-}$ is equivalent to the additional spin precession angle Ω of the tunneling (transmitted) neutron.

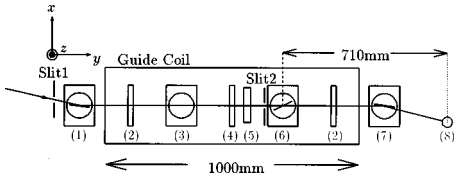

FIG. 2. Schematic layout of the neutron spin interferometer at JRR-3M. (1) Polarizer, (2) $\pi/2$ spin flipper coil, (3) precession coil I(PC1), (4) π spin flipper coil, (5) accelerator coil, (6) precession coil II(PC2) and a magnetic film (sample), (7) analyzer, (8) ^{3}He detector.

B. Measurement of the additional Larmor precession angle by means of the NSE method

The essential features of the NSE method proposed by Mezei [13] have been well explained with the classical image of Larmor precession of the neutron spin, and the intensity of the NSE signal is given as a function of the δN, which is the difference between the numbers of Larmor precession before and after the π flipper coil. In our configuration shown in Fig. 2, δN is described by

$$\delta N=N_0-N_1-N_2-\Delta N=\frac{\gamma_L}{2\pi}\left(\frac{H_0l_0}{v_0}-\frac{H_1l_1}{v_1}-\frac{H_2l_2}{v_1}\right)-\Omega/2\pi, \tag{2.8}$$

where $\gamma_L=2\mu/\hbar=29.16$ kHz/mT, ΔN is the additional Larmor precession turn due to the magnetic film, N the number of Larmor precession, l the length of the magnetic field H, and v the neutron velocity. The subscripts 0, 1, and 2 indicate the situations in the precession coil I(PC1), the precession coil II(PC2), and the accelerator coil, respectively.

Figure 3 shows the typical NSE signal without the sample. In this experiment, H_0, H_1, l_0, l_1, and l_2 are constant. The NSE signal is, hence, measured as a function of the current H_2 of the accelerator coil. One period of the signal corresponds to one turn of Larmor precession. In transmission experiments, $v_0=v_1$, therefore, a shift of NSE signals with and without the magnetic film at an incident angle is equivalent to an average additional angle of Larmor precession of neutrons through the magnetic film at the incident angle. Thus, the additional Larmor precession angles due to the magnetic film are precisely derived from the shifts of the NSE signals as a function of the incident angles.

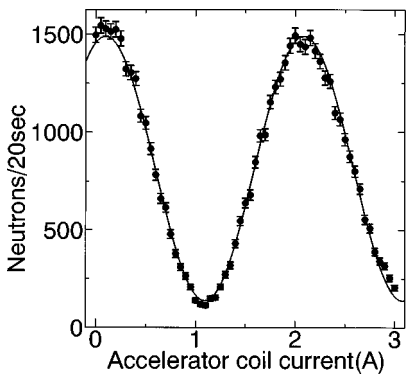

FIG. 3. Typical NSE signal measured as a function of accelerator coil current.

III. EXPERIMENTAL PROCEDURES

We have prepared four magnetic films with thickness 200, 300, 400, and 3900 Å. The thickest film was used to estimate the applicable range for Larmor precession as a clock. The other thin films were used to measure the additional spin precession angles in the tunneling process.

The material of the magnetic films is Permalloy45 ($Fe_{55}Ni_{45}$), which is magnetically soft. The magnetic films were evaporated on a polished silicon wafer in an applied magnetic field of 14 mT in order to saturate the films under lower magnetic field [19,20]. The dimension of the silicon wafer for thickness 3900 Å was a rectangular slab 130 mm wide, 65 mm high, and 0.6 mm thick, and those 200–400 Å thick were disks 75 mm in diameter and 3 mm thick, respectively. The experiments on thicker film (3900 Å) were carried out with the transverse NSE spectrometer (NSE-KURRI) [21] installed on a CN3 guide tube at the Research Reactor Institute Kyoto University (KURRI), and that of thinner films 200–400 Å thick were carried out with the cold neutron spin interferometer (NSI-JAERI) [22] installed at the C3-1-2 beam port of the JRR-3M reactor at the Japan Atomic Energy Research Institute (JAERI). The incident wavelength resolution and the divergent angle were 5.8 Å ± 0.67 Å [full width at half-maximum (FWHM)] and 1.0×10^{-3} rad, for the NSE-KURRI, respectively; 12.6 Å ± 0.44 Å and 0.7×10^{-3} rad for the NSI-JAERI, respectively. The neutron velocities of wavelengths 5.8 and 12.6 Å correspond to 682 and 314 m/s, respectively. The strength of the magnetic field at sample position (PC2) for the NSI-JAERI was 2mT and that for the NSE-KURRI was 8 mT. Neutron intensity, wavelength, and its resolution at the NSI-JAERI are far superior to those at the NSE-KURRI; however, the magnetization of the thick film was not saturated at the NSI-JAERI. Therefore we used the NSE-KURRI to measure the additional Larmor precession angle of neutron across the magnetic thicker film for the nontunneling case. On the other hand, it was possible to saturate the magnetization of the thin films at the NSI-JAERI. Therefore we used the NSI-JAERI for the tunneling case.

For the simulation of the relative phase difference of ↑ and ↓ spin, it is necessary to evaluate the correct values of average nuclear and magnetic potential in the magnetic film. These potential values can be estimated by least-squares fitting of the measured transmission probabilities of ↑ and ↓ spin neutron through the film with simulation. The transmission experiments were carried out with configurations of the NSE-KURRI and NSI-JAERI without the analyzer.

IV. EXPERIMENTAL RESULTS AND DISCUSSIONS

A. Transmission probabilities of ↑ and ↓ spin neutrons through the magnetic film

Figures 4(a) and 4(b) show the transmission probabilities of ↑ and ↓ spin neutrons through the magnetic Permalloy45 film with thickness 3900 Å and through only silicon substrate, respectively, as a function of the incident angle at the NSE-KURRI. The closed and open circles indicate experimental transmission probabilities of ↑ and ↓ spin neutrons, respectively. As shown in Fig. 4(a), transmission probabilities of ↑ and ↓ spin neutron through the silicon substrate

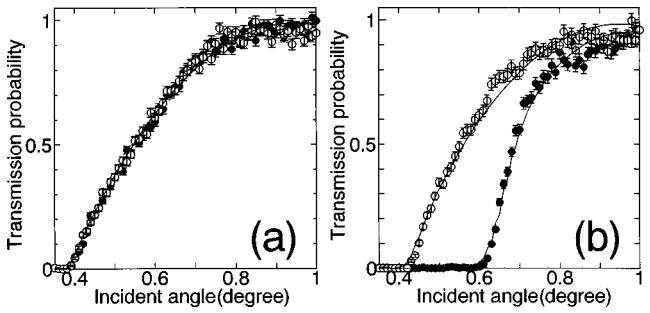

FIG. 4. Transmission probabilities of ↑ and ↓ spin neutrons through (a) only the silicon substrate without the Permalloy45 film and (b) the Permalloy45 film with thickness 3900 Å at the NSE-KURRI.

agree with each other. Therefore the substrate does not affect the Larmor precession angle. As shown in Fig. 4(b), the experimental transmission probabilities of ↑ and ↓ spin neutrons are well reproduced by the theoretical lines. The theoretical lines are calculated from Eq. (2.3) including effects of the incident wavelength distribution at the NSE-KURRI and the experimental transmission probability through only silicon substrate shown in Fig. 4(a). The average nuclear and magnetic potential values for the best fitting were 218 and 84.4 neV, respectively, and the magnetic potential corresponds to 1.4 T.

Figure 5(a) shows transmission probabilities of ↑ and ↓ spin neutron through only silicon substrate, Figs. 5(b)–5(d) shows them through the magnetic films with thicknesses 200, 300, and 400 Å, respectively. The closed and open circles indicate experimental transmission probabilities of ↑ and ↓ spin neutrons, respectively. These results are also well reproduced by the theoretical lines calculated from Eq. (2.3) including the effects of incident wavelength distribution at the

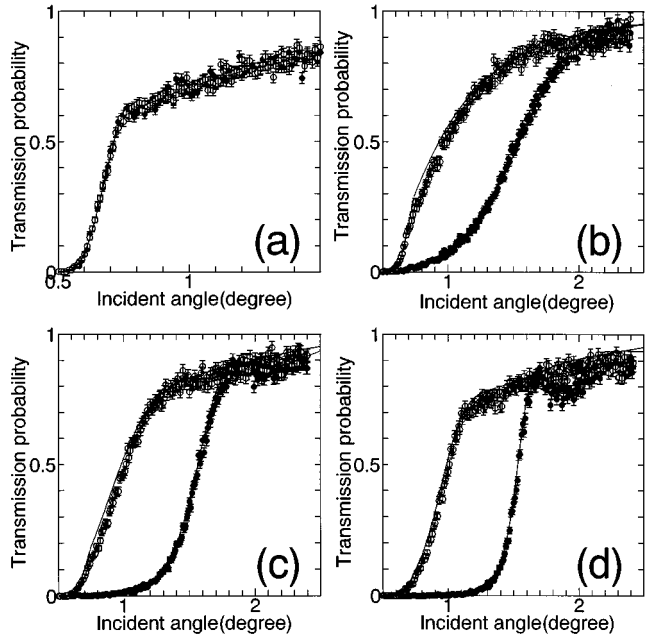

FIG. 5. Transmission probabilities of ↑ and ↓ spin neutrons through (a) only the silicon substrate without the Permalloy45 film and through the Permalloy45 films with thicknesses (b) 200, (c) 300, and (d) 400 Å at the NSI-JAERI.

TABLE I. Measured parameters of the magnetic films in transmission experiments.

Thickness (Å)	V_{nucl} (neV)	$\lvert\mu B\rvert$ (neV)	B (T)	$\theta_{c(\uparrow)}$ (deg.)	$\theta_{c(\downarrow)}$ (deg.)	$\theta_{c(\mathrm{Si})}$ (deg.)	λ (Å)	Instrument
200	214	93.5	1.55	1.40	0.88	0.59	12.6	NSI-JAERI
300	212	96.5	1.60	1.40	0.86	0.59	12.6	NSI-JAERI
400	212	96.5	1.60	1.40	0.86	0.59	12.6	NSI-JAERI
3900	218	84.4	1.40	0.64	0.42	0.27	5.8	NSE-KURRI

NSI-JAERI and the experimental transmission probability of silicon substrate as shown in Fig. 5(a). The minimum incident angle covering the neutron beam width was estimated to be 0.48°. The values of average nuclear and magnetic potentials evaluated in Figs. 4 and 5 are shown in Table I. $\theta_{c(\uparrow)}, \theta_{c(\downarrow)}$, and $\theta_{c(\mathrm{Si})}$ indicate the critical angle of total reflection for $\uparrow,\downarrow$ spin neutron and the critical angle of silicon at the incident wavelength λ, respectively. In Table I, a slight deviation of the potential values was observed. The deviation might be the result of the deviation of concentration of iron and nickel in the films. Here the average nuclear and magnetic potentials for iron are 209 and 131 neV, respectively; those for nickel are 245 and 38.5 neV, respectively. Since the length of the silicon substrate is 75 mm and the thickness is 3.0 mm, at the incident angles below 2.3° (3/75 rad), all neutrons through the substrate come from the edge of the substrate. The direction of the neutrons from the edge of the substrate slanted θ_Δ to the incident neutron beam direction, where θ_Δ is the difference between the incident angle and the refractive angle in the substrate. θ_Δ increases with smaller incident angle. Therefore the intensities of neutrons as shown in Fig. 5(a) are reduced at the incident angles below 0.75° though the critical angle of silicon substrate for the incident wavelength of 12.6 Å is 0.59°.

B. Measured NSE signals through the magnetic films

In the vicinity of the critical angle of silicon, as described in Sec. IV A, the neutrons going out from the edge of the substrate are not detectable at the analyzer position shown in Fig. 2. Therefore we moved the analyzer 2.0 mm along x direction shown in Fig. 2 to measure NSE signals at the incident angles below 0.90°. The difference of number of Larmor precession between the two configurations is given by

$$\delta N' = \frac{\sqrt{l_A^2+2^2}-l_A}{l_A} N_A < \frac{4.7\times 10^{-3}}{425} 18 \simeq 2.0\times 10^{-4}, \tag{4.1}$$

where l_A is the distance between the film and the analyzer shown in Fig. 2, N_A is number of Larmor precession between the film and the second $\pi/2$ flipper coil. Therefore the effect of change of the configuration is negligible.

Figures 6(a) and 6(b) show spin echo signals of neutrons transmitted through the magnetic film with thickness 200 Å at incident angles of 5.0° and 1.0°, respectively, (c) and (d) show that with a thickness of 400 Å at incident angles of 5.0° and 1.0°, respectively. As shown in Figs. 6(b) and 6(d), NSE signals were observed at the incident angle of 1.0,° which is in the tunneling region for the ↑ spin neutron. We confirmed, therefore, that coherent superposition between the tunneling ↑ spin and nontunneling ↓ spin neutron is still conserved. Though the polarizations of the NSE signal shown in Figs. 6(a) and 6(c) are almost identical, the polarization of the NSE signal in Figs. 6(d) is much smaller than that in Figs. 6(b). The reduction of the polarization of the NSE signal occurred as a result of a large difference of the transmission (tunneling) probabilities of ↑ spin neutrons for thickness 200 Å and 400 Å. The normalized polarization of the NSE signal P_{NSE} for a monochromatic beam can be written as

$$P_{\mathrm{NSE}} = P_{\mathrm{s}} \frac{\lvert\langle S_{\mathrm{xy}};\mathrm{tr}\rangle\rvert}{\lvert\langle S_{\mathrm{xy}};\mathrm{tr}\rangle\rvert + \frac{1}{2}\lvert\langle S_{\mathrm{z}};\mathrm{tr}\rangle\rvert} = P_{\mathrm{s}} \frac{4\sqrt{T_+T_-}}{4\sqrt{T_+T_-}+\lvert T_+ - T_-\rvert}, \tag{4.2}$$

where $\lvert\langle S_{\mathrm{xy}};\mathrm{tr}\rangle\rvert = \sqrt{\langle S_{\mathrm{x}};\mathrm{tr}\rangle^2+\langle S_{\mathrm{y}};\mathrm{tr}\rangle^2}$, $P_{\mathrm{s}} \simeq 1/0.83$ the inverse of polarization of the NSE signal without a magnetic film as shown in Fig. 3. In practice, the NSE signal shown in Fig. 6(d) was observed even if the ratio of transmission probabilities (T_+/T_-) was below 1/400. Thus this method using

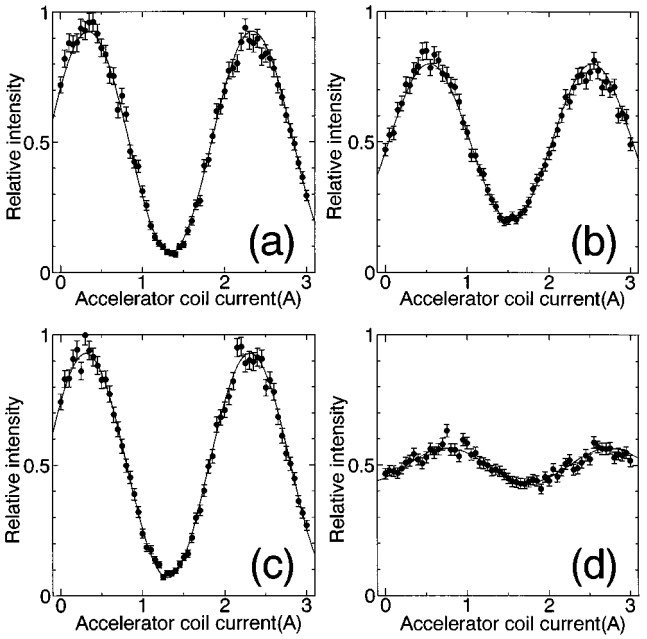

FIG. 6. NSE signals through the Permalloy45 films with thickness 200 Å at (a) 5.0° and (b) 1.0°, and with thickness 400 Å at (c) 5.0° and (d) 1.0° for the NSI-JAERI. The incident angle of (b) and (d) is below the critical angle of the ↑ spin neutron and is above that of the ↓ spin.

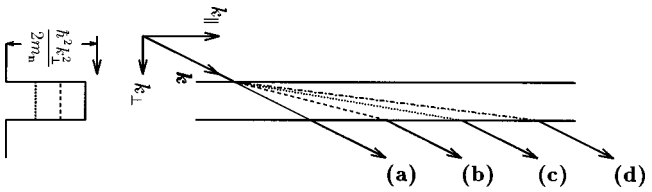

FIG. 7. Schematic view of classical neutron paths due to refractions in a magnetized film. (a) passing without refraction, (b) refraction path of the ↓ spin neutron, (c) refraction path due to only nuclear potential, and (d) refraction path of the ↑ spin.

spin interference is suitable for measuring the Larmor precession angles even in the vicinity of the critical angle of silicon.

C. Additional spin precession angles through the magnetic films

1. Nontunneling case

Let us consider the classical path of a Larmor precessing neutron in a magnetized film for the nontunneling case. A refraction angle of ↑ spin neutron is smaller than that of the ↓ spin neutron. The path of the ↑ spin neutron in the film is, therefore, longer than that of the ↓ spin, and the classical paths are shown in Fig. 7. In Fig. 7, (a) is the path without refraction, (b) the path of the ↓ spin neutron, (c) the path due to average nuclear potential in the film, and (d) the path of the ↑ spin one. We experimentally investigated whether or not the Larmor precessing neutron in the film was defined by one classical traversal path.

Figures 8 show shifts of spin echo signals of neutrons transmitted through the film with a thickness of 3900 Å. The closed circles are measured shifts of the NSE signals and were obtained by least-squares fitting a cosine function to the NSE signals. In Fig. 8, the lines (a)–(d) indicate classical Larmor precession angles Ω_c derived from the Larmor frequency and traversal time for the neutron transmitted through four classical paths (a)–(d) shown in Fig. 7, respectively. The classical precession angle is given by

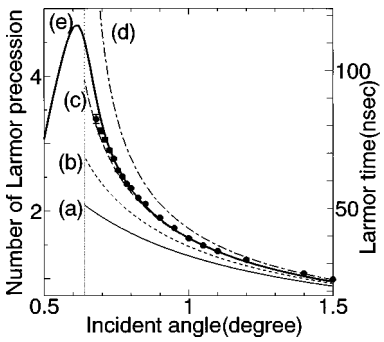

FIG. 8. The shift of NSE signals through the Permalloy45 film with thickness 3900 Å. The closed circles were measured; the various lines (a)–(d) were classical Larmor precession angles calculated from the Larmor frequency ω_L and neutron paths (a)–(d) in Fig. 7, respectively. The bold solid line (e) indicate the spin precession angle calculated from the stationary states for the rectangular barrier. The broken vertical line indicates the critical angle of the ↑ spin neutron with a wavelength of 5.8 Å.

$$\Omega_c = \gamma_L B l_n/v_n - \gamma_L H l_n/v_n \simeq \gamma_L B l_n/v_n = \omega_L (l_n/v_n) = \omega_L \tau_T, \tag{4.3}$$

$$B \simeq 1.4\times 10^3 \gg H \simeq 8 \text{ mT},$$

where $\omega_L \simeq 2.57\times 10^8$ rad/sec, v_n is neutron velocity in the film, and l_n is one of path lengths of (a)–(d) shown in Fig. 7. The measured Larmor precession angles are well interpreted as the products of the Larmor frequency ω_L and traversal times τ_T that a neutron spends in the path (c) of Fig. 7, and they are also well reproduced by the theoretical line (*e*) calculated from Eqs. (2.5)–(2.7). When the incident angle is sufficiently larger than the critical angle, the spin precession angle predicted with the stationary state is equivalent to the Larmor precession angles, which are productions of the Larmor frequency and the traversal time associated with the classical path due to the average nuclear potential in the film.

To consider the effect of only the first order of the magnetic field, the Larmor precession angle in the nontunneling case $[E_\perp \geqslant (V_{\text{nucl}} + \mu B)]$ is described as

$$\Omega = |\Delta\phi_+ - \Delta\phi_-| = (k_- - k_+)d = k_0[(1+\epsilon)^{1/2} - (1-\epsilon)^{1/2}]d \simeq \epsilon k_0 d = \omega_L d/v_\perp = \omega_L \tau_T, \tag{4.4}$$

where $k_\pm = i\kappa_\pm$, $k_0 = \sqrt{2m_n(E_\perp - V_{\text{nucl}})}/\hbar$, $v_\perp = \hbar k_0/m_n$, $\epsilon = \mu B/|E_\perp - V_{\text{nucl}}|$, and $\omega_L = 2\mu B/\hbar$. Thus the Larmor precession can be used as a clock to measure the traversal time τ_T of neutron across the film for the approximate parameter $\epsilon \ll 1$. As described in Sec. I, the Larmor time is defined by dividing the additional Larmor precession Ω with the Larmor frequency ω_L. Therefore, when ϵ is sufficiently smaller than 1, the Larmor time is equal to the traversal time.

The deviation of the Larmor time and the traversal time increases with smaller incident angle. At the minimum incident angle (0.68°), the measured Larmor time is estimated to be 81.5 ± 1.8 nsec and the approximate parameter ϵ is 0.68. In this case, ϵ is not sufficiently small. Therefore we consider the effect of magnetic induction of the film to fifth order and then the Larmor precession angle is given by $\Omega \simeq \omega_L(1+\epsilon^2/8+7\epsilon^4/128)\tau$. The deviation of the Larmor time and the traversal time is calculated to be 6.9% for $\epsilon = 0.68$, and the Larmor time can be interpreted as the traversal time with an error of less than 10%. Thus we have experimentally confirmed that the Larmor precessing neutron across the film passes along the path due to average nuclear potential in the film, and that the Larmor time corresponds to the traversal time of a neutron across the film for $\epsilon \ll 1$. Here the change of neutron velocity in a vacuum (air) and the film is of order 10^{-5}. The real traversal time can be, therefore, interpreted as a function of the average traversal path length of neutrons across the film when the incident angle is much larger than the critical angle.

2. Tunneling case

Figures 9(a) and 9(b) show the shift of spin echo signals of neutrons through the Permalloy45 thin film with a thickness of 200 Å. The NSE signals were observed down to the incident angle of 0.62° below the critical angles of both the

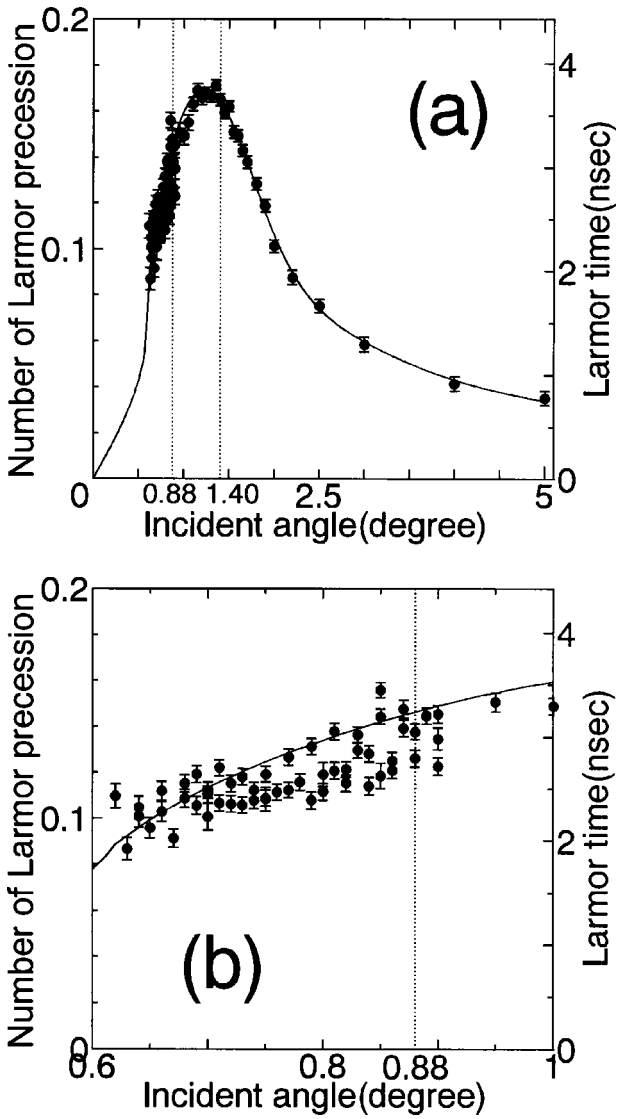

FIG. 9. The shift of NSE signals through the Permalloy45 film with thickness 200 Å as a function of the incident angle (a) from 0° to 5.0° and (b) from 0.6° to 1.0°. The closed circles are measured and the solid lines are the spin precession angles calculated from the stationary states for the rectangular barrier. These broken vertical lines indicate the critical angles of ↑ and ↓ spin neutrons with a wavelength of 12.6 Å, respectively.

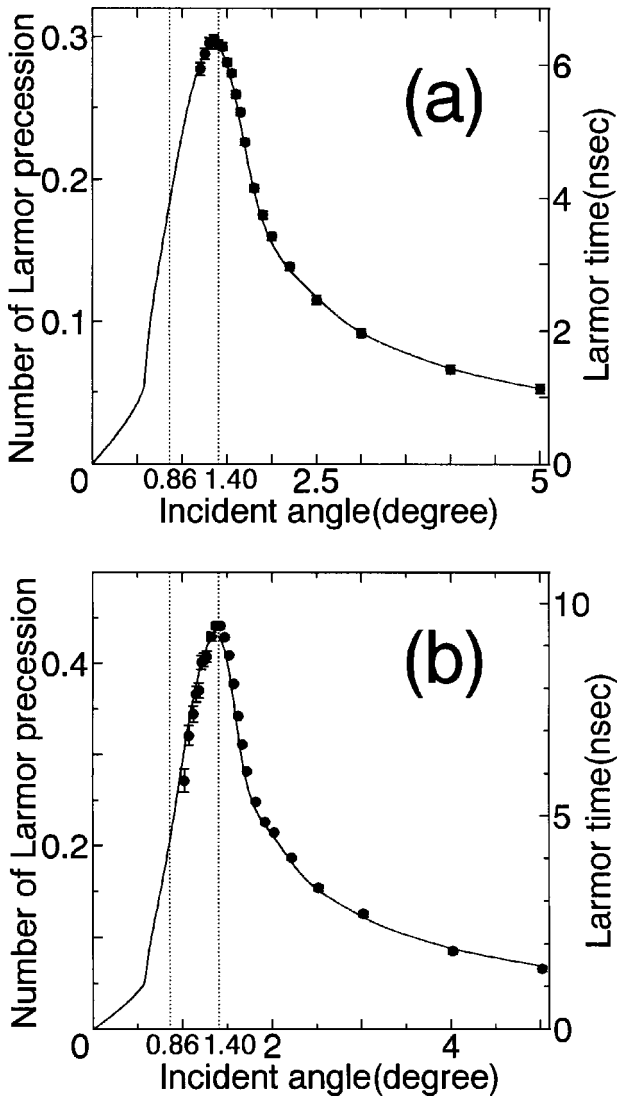

FIG. 10. The shift of NSE signals through the Permalloy45 films with thicknesses (a) 300 and (b) 400 Å as a function of the incident angles. The closed circles are measured and the solid lines are the spin precession angles calculated from the stationary states for the rectangular barrier. These broken vertical lines are the critical angles of ↑ and ↓ spin neutron of wavelength 12.6 Å, respectively.

↑ and ↓ spin neutrons. In the tunneling region of the incident angles below the critical angles of both the ↑ and ↓ spin neutrons, the smaller the incident angle is, the less the spin precession angle is. The spin precession reaches the maximum value between the critical angles of the ↑ and ↓ spin neutrons, and it is in proportion to inverse of the normal component of the wave vector. Even in the tunneling region, the measured closed circles were well reproduced by the theoretical line calculated from Eqs. (2.5)–(2.7). Thus, the spin precession angle of the tunneling neutron is also represented with the relative phase difference of the ↑ and ↓ spin neutron wave functions derived by solving the one-dimensional Schrödinger equation.

Figures 10(a) and 10(b) show the shift of spin echo signals of neutrons transmitted through the Permalloy45 thin film with thicknesses of 300 and 400 Å, respectively. As well as Fig. 9, the measured closed circles were well reproduced the theoretical line calculated from Eqs. (2.5)–(2.7). In the incident angles from 0.85° to 1.41°, the additional spin precession is represented as coherent superposition between the tunneling ↑ spin neutron and the nontunneling ↓ spin neutron. Comparing Fig. 9 with Fig. 10, it is shown that the spin precession is proportional to the thickness.

Let us extract Larmor times from the measured spin precession angles. In the thinnest film of thickness 200 Å, the Larmor frequency ω_L is estimate to be 2.84×10^8 (rad/s) and the Larmor time is shown in the right ordinate of Fig. 9. In the films of thicknesses 300 and 400 Å, the Larmor frequencies are 2.93×10^8 rad/s and the Larmor times are shown in the right ordinates of Figs. 9 and 10, respectively. The spin precession angle in the tunneling case $[E_\perp \leqslant (V_{\mathrm{nucl}}-\mu B)]$ is described as

$$\Omega = |\Delta\phi_+ - \Delta\phi_-| = (\kappa_+ - \kappa_-)d = \kappa_0[(1-\epsilon)^{1/2} - (1+\epsilon)^{1/2}]d \simeq \epsilon\kappa_0 d = \omega_L d/v'_\perp = \omega_L \tau'_T, \quad (4.5)$$

where $\kappa_0 = \sqrt{2m_n(V_{nucl} - E_\perp)}/\hbar, v'_\perp = \hbar\kappa_0/m_n$.

At the minimum incident angle (0.62°), the Larmor time τ'_T is estimated to be 2.42 ± 0.12 nsec and the approximate parameter ϵ is 0.61. Although the meaning of $v_\perp$ is clearly interpreted as the actual normal neutron velocity for the nontunneling case, that of $v'_\perp$ cannot be considered as any actual neutron velocity for the tunneling case. Thus, the definition of the Larmor clock for the tunneling case does not have, strictly speaking, an acceptable basis [3], and then it is not clear whether the Larmor time corresponds to the tunneling time associated with the question ''How long does it takes for a particle to tunnel through a barrier?''

Several authors have suggested that the effects of a wave packet be considered for the measurement of the tunneling time of a particle [2–4]. Recently, Krenzlin and co-workers numerically investigated tunneling of wave packets using a time-dependent Schrödinger equation and showed how the Larmor clock works during the tunneling process [23]. They indicated that the Larmor time agreed with the stationary-state prediction for wide spatial spread wave packets. According to their results, the wave packets of neutrons at the NSI-JAERI are wide spatial spread in comparison with the thicknesses of the films. However, the concept of a wide spatial spread neutron is different from that of a classical particle. Thus we have no answer to the classical question about the tunneling time though spin precession angles of tunneling neutrons have been precisely measured. According to the theory of tunneling time using Nelson's stochastic approach by Imafuku and co-workers [24], the deviation of the experimental values shown in Fig. 9(b) corresponds to their tunneling time. In the measurements of this study, we have not extracted their tunneling time due to a little instability of the NSI-JAERI.

V. CONCLUSIONS

In this paper, the spin precession angles of neutrons tunneling and nontunneling through the Permalloy45 ($Fe_{55}Ni_{45}$) ferromagnetic film have been precisely measured as a function of the incident angles. In both tunneling and nontunneling cases, the additional spin precession angles were well reproduced by the relative phase difference between the $\uparrow$ and $\downarrow$ spin neutron wave functions that were derived by solving the one-dimensional Schrödinger equation for the optical potentials in the film. Though the ratio of the transmission probabilities of $\uparrow$ and $\downarrow$ was below 1/400, the additional spin precession angles were precisely observed by means of the spin interference.

The Larmor times have been extracted from the additional spin precession for tunneling and nontunneling cases. For the nontunneling case, we have experimentally confirmed that classical path of Larmor precessing neutron across the film can be interpreted as the path due to average nuclear potential V_{nucl} in the film, and that the Larmor time corresponds to traversal time of a neutron across the film for the approximate parameter $\epsilon = \mu B/|E_\perp - V_{nucl}| \ll 1$. For the tunneling case, the Larmor times agree with the stationary-state prediction, thus we have found no evidence that the Larmor time corresponds to the tunneling time it takes for a particle to tunnel through the barrier.

ACKNOWLEDGMENTS

This work was supported by the interuniversity program for the KURRI and JAERI facilities, and financially by the Yamada Science Foundation and a Grant-in-Aid for Scientific Research from the Japanese Ministry of Education, Science and Culture (Grant Nos. 04244103, 06220203, 07209202, and 08874019). One of the authors (M.H.) was supported by JSPS.

[1] M. Büttiker, Phys. Rev. B **27**, 6178 (1983).
[2] S. Collins, D. Lowe, and J. R. Barker, J. Phys. C **20**, 6213 (1987); **20**, 6233 (1987).
[3] E. H. Hauge and J. A. Støvneng, Rev. Mod. Phys. **61**, 917 (1989).
[4] J. P. Falck and E. H. Hauge, Phys. Rev. B **38**, 3287 (1988).
[5] R. Landauer and Th. Martin, Rev. Mod. Phys. **66**, 217 (1994).
[6] A. I. Baz', Yad. Fiz. **4**, 252 (1966) [Sov. J. Nucl. Phys. **4**, 182 (1967)]; **5**, 299 (1966) [**5**, 161 (1967)].
[7] V. F. Rybachenko, Yad. Fiz. **5**, 895 (1966) [Sov. J. Nucl. Phys. **5**, 635 (1967)].
[8] P. Gueret, A. Baratoff, and E. Marclay, Europhys. Lett. **3**, 367 (1987).
[9] M. Deutsch and J. E. Golub, Phys. Rev. A **53**, 434 (1996).
[10] Ph. Balcou and L. Dutriaux, Phys. Rev. Lett. **78**, 851 (1996).
[11] M. Hino, N. Achiwa, S. Tasaki, T. Ebisawa, T. Akiyoshi, and T. Kawai, J. Phys. Soc. Jpn. Suppl. A **65**, 201 (1996); **65**, 277 (1996).
[12] N. Achiwa, M. Hino, S. Tasaki, T. Ebisawa, T. Akiyoshi, and T. Kawai, J. Phys. Soc. Jpn. Suppl. A **65**, 181 (1996).
[13] *Neutron Spin Echo*, edited by F. Mezei, Lecture Notes in Physics Vol. 128 (Springer, Heidelberg, 1980).
[14] *Neutron Interferometry*, edited by U. Bonse and H. Rauch (Clarendon Press, Oxford, 1979).
[15] J. Summhammer, G. Badurek, H. Rauch, U. Kischko, and A. Zeilinger, Phys. Rev. A **27**, 2523 (1983).
[16] For example, W. Gavin Williams, *Polarized Neutron* (Clarendon Press, Oxford, 1988).
[17] S. Yamada, T. Ebisawa, N. Achiwa, T. Akiyoshi, and S. Okamoto, Annu. Rep. Res. Reactor Inst. Kyoto Univ. **11**, 8 (1978).
[18] V. F. Sears, *Neutron Optics* (Oxford University Press, New York, 1989).
[19] S. Tasaki, T. Ebisawa, T. Akiyoshi, T. Kawai, and S. Okamoto, Nucl. Instrum. Methods Phys. Res. A **355**, 501 (1995).
[20] T. Kawai, T. Ebisawa, S. Tasaki, Y. Eguchi, M. Hino, and N. Achiwa, J. Neutron Res. **5**, 123 (1997).

[21] M. Hino, N. Achiwa, S. Tasaki, T. Ebisawa, and T. Akiyoshi, Physica B **213&214**, 842 (1995).

[22] T. Ebisawa, H. Funahashi, S. Tasaki, Y. Otake, T. Kawai, M. Hino, N. Achiwa, and T. Akiyoshi, J. Neutron Res. **4**, 157 (1996).

[23] H. M. Krenzlin, J. Budczies, and K. W. Kehr, Phys. Rev. A **53**, 3749 (1996).

[24] K. Imafuku, I. Ohba, and Y. Yamanaka, Phys. Rev. A **56**, 1142 (1997).